Development of Power Spectral Techniques for Design of Aircraft to Gusts

JOHN C. HOUBOLT

Aeronautical Research Associates of Princeton, Inc.
50 Washington Road, Princeton, New Jersey, U.S.A.

ABSTRACT

Results of a study aimed at the development of gust design procedures based on power spectral techniques are presented. The treatment includes a description of atmospheric turbulence make-up, and a discussion of the aircraft structural parameters that are needed in spectral evaluation procedures. Ease of application, interpretation and implication to design, present and future, and comparison with past design procedures are covered. A special feature shows the spectral deductions that can be made from past discrete gust design. The necessity and means for obtaining and reducing data of routine and test flights in a more meaningful, consistent and useful way are also touched upon.

1. INTRODUCTION

Throughout the aircraft industry there is much interest in the development of power spectral procedures for designing aircraft for gust encounter. In England, Zbrozek, Burns, Bullen, Burnham *et al.*, have made significant contributions in spectral developments, and counterpart personnel are found in the United States and other countries. In the United States the FAA has sponsored a study toward the development of spectral procedures for civilian aircraft, and the Air Force has a current programme for military type aircraft. References 1, 2, and 3 summarise some of the developments that have been made to date in the Air Force programme. Four possible and promising approaches are brought out in these references. It is the purpose of this report to single out one of these approaches. The approach is highlighted here because it conceptually has the simplicity of the discrete gust

design approach and further, because of its ease of application. An aim is to attempt to obtain input from other countries to help evaluate and firm up the approach. A section is included which shows the possibilities of obtaining spectral design limits based on discrete gust design.

Symbols

a	lift curve slope
A	structural response parameter ($\sigma_x = A\sigma_w$)
c, c_0	wing chord
$F(k)$	in phase oscillatory lift coefficient
g	acceleration of gravity
$G(k)$	out-of-phase oscillatory lift coefficient
H	gust gradient distance
$H(\omega)$	frequency response function
k	reduced frequency parameter ($k = \omega c/2V$)
K_g	gust alleviation factor
L	gust scale length
Δn	incremental load factor
N	number of upward crossings per second
N_0	number of upward zero crossings per second
P	proportion of time in turbulence
S	wing area
U_{de}	equivalent gust velocity
V	airspeed
V_e	equivalent airspeed
W	weight
Δx	incremental response due to gusts
μ_g, μ_0	mass parameters ($\mu_0 = 4\mu_g$)
ρ	air density
ρ_0	sea level air density
σ	r.m.s. value
σ_c	composite r.m.s. gust velocity
σ_w	r.m.s. gust velocity
$\phi(\omega)$	power spectrum
ω	angular frequency
Ω	spacial frequency ($\Omega = \omega/V$)

2. Basic Spectral Equations

The basic relation used herein between the input gust spectrum ϕ_w and the output response spectrum ϕ_x is:

$$\phi_x(\omega) = |H(\omega)|^2 \phi_w(\omega) \tag{1}$$

where x is any dynamic response quantity of concern and H is the frequency response function for x due to unit sinusoidal gusts. Uniform gust loading in the spanwise direction is implied. From eqn. (1) two basic structural response quantities are found by the equations

$$A = \frac{1}{\sigma_w}\left[\int_0^{\omega_c} \phi_x(\omega)\,\mathrm{d}\omega\right]^{1/2} = \frac{\sigma_x}{\sigma_w}$$

$$N_0 = \frac{1}{2\pi}\left[\frac{\int_0^{\omega_c} \omega^2 \phi_x(\omega)\,\mathrm{d}\omega}{\int_0^{\omega_c} \phi_x(\omega)\,\mathrm{d}\omega}\right]^{1/2}$$

where A, as shown, relates the r.m.s. value σ_w of gust input to the r.m.s. value σ_x of output response according to the equation

$$\sigma_x = A\sigma_w \tag{2}$$

and where N_0 is the number of times per second the output time history crosses zero with positive slope. The upper limit of integration ω_c as used in the definitions is somewhat arbitrary, but for convenience and minimum of work may be taken simply as the point where A and N_0 remain essentially unchanged with increasing ω_c. In some cases N_0 may not level off, and in these instances the rule of thumb suggested is to choose ω_c as the point where A has become essentially constant.

3. Simplified Gust Design Based on A and N_0

In ref. 1, the development of a 'universal' curve for load exceedances is given (*see* ref. 4 also). One such curve is shown in Fig. 1; it applies to any response variable x of concern, such as stress, bending moment, acceleration, etc., where Δx is the increment in response due to gust encounter. A limit load reference for design will be followed herein such that

$$\Delta x = x_{LL} - x_{1-g}$$

Other parameters are: N is the number of times per second that the response level Δx is crossed with positive slope, P is the total proportion of flight time spent in turbulence, and σ_c is a composite r.m.s. value of all the σ_w's encountered.

At least four design procedures may be developed from this universal curve, as outlined in ref. 2. Here however only one is featured. It follows

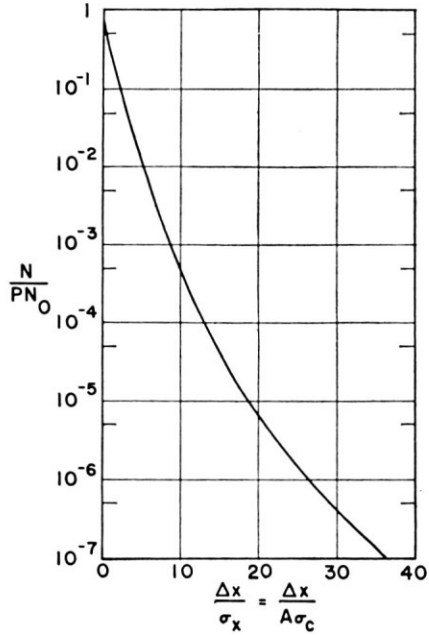

FIG. 1 — 'Universal' curve for load exceedance

rather easily from Fig. 1 by making the assumption that N, P, and σ_c are the same for all aircraft; this assumption is very much analogous to the use of a fixed U_{de} in the discrete-gust-design approach used in the past. With N, P, and σ_c constant, Fig. 1 indicates the functional relation

$$N_0 = f(\Delta x/A) \tag{3}$$

One way to establish f is to specify values of N, P, and σ_c and then use the universal curve to establish directly the variation of N_0 with $\Delta x/A$; this approach supposes a well-founded universal curve, and a sound basis for choosing N, P, and σ_c. Another way is an empirical approach as follows. Suppose values of N_0 and $\Delta x/A$ are computed for a number of existing gust critical aircraft which have proven themselves airworthy through many years of successful operation. These values when plotted would lead to the shotgun type pattern shown in Fig. 2. A border of the type indicated by eqn. (3) may then be drawn along the leftmost points as shown, guided in general slope characteristics by the behaviour of the universal curve, with the inference that design points falling below this line represent safe design. It is to be noted that in this empirical construction all considerations of N, P, and σ_c are suppressed or eliminated.

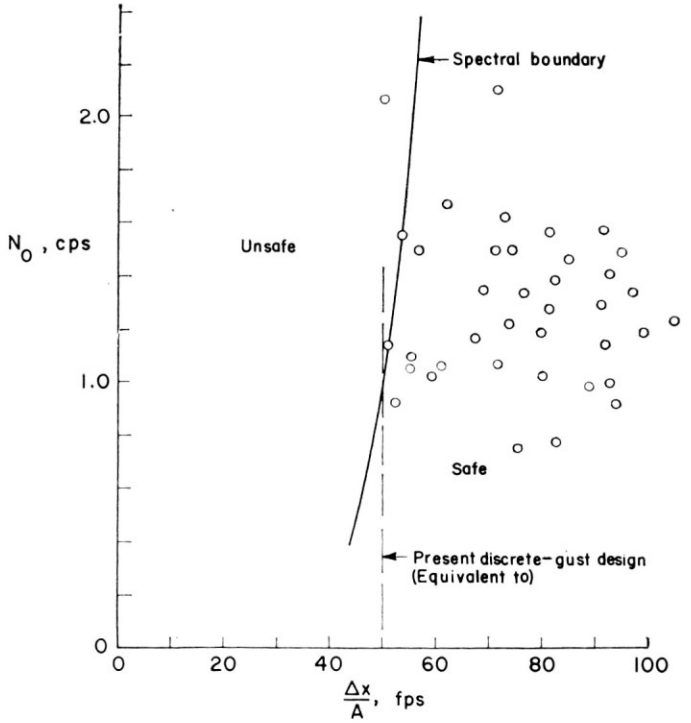

FIG. 2 — N_0 versus $\Delta x/A$ design approach (points and boundary are illustrative)

The points and line shown in Fig. 2 are illustrative in nature and do not represent any computed values. However, calculations of $\Delta x/A$ and N_0 for certain aircraft are being made for the Air Force by some of the aircraft companies. These calculated values are to be used in helping to establish the definite position of a design border. It would appear desirable to obtain similar values for British and other aircraft to see if they support the pattern.

Figure 2 represents the very heart of this paper. With such a figure established, gust design by spectral technique is seen to be very easy and straightforward. All that has to be done is to calculate N_0 and $\Delta x/A$, and to plot the point on the figure to see if it falls on the safe side. It is of interest to note that in terms of stress at a point, adding metal lowers the associated A (the value of N_0 is probably changed only very little). Thus if a point fell to the left of the border, the addition of metal would lower A and hence move the point to the right. Actually this procedure bears a close resemblance to the discrete gust design approach, but with two basic and noteworthy improvements. The first improvement is associated with the $\Delta x/A$ axis. Values along

this axis are the equivalent counterpart to U_{de}, the gust velocity value used in discrete gust design. To see this, consider

$$\sigma_x = A\sigma_w$$

and multiply both sides by η so that $\eta\sigma_x$ becomes equal to Δx_d, the design value of Δx, then

$$\frac{\Delta x_d}{A} = \eta\sigma_w = U_d$$

By contrast, a similar relation by the discrete gust design approach would appear

$$\frac{\Delta x_d}{A_{de}} = U_{de}$$

indicating that U_d is similar in concept to U_{de}. The discrete gust design procedure is thus represented in Fig. 2 by a fixed vertical line, as indicated. The newer approach discussed here not only allows a variation in U_d but establishes the value more accurately since A is determined by the more refined spectral relations compared to the establishment of A_{de}, which is based primarily on the K_g curve[5].

The second improvement is that of the N_0 axis. In the discrete gust approach, no explicit account is taken of the number of times gusts load levels are encountered. The N_0 axis effectively takes this fact into account explicitly. Thus, in short, the boundary design curve of Fig. 2 reflects that a trade-off between the A and N_0 value is possible in design; specifically, for example, increasing N_0 must be accompanied by decreasing A.

In the next section, two rigid body treatments are given, one along spectral lines and one from a discrete gust point of view. A comparison of results leads to a finding which is remarkably similar to the result shown in Fig. 2. This finding may thus represent a possible further means to help establish the position of the design boundary line on Fig. 2.

4. Spectral Design Limits Based on Discrete Gust Design

A rigid aeroplane with a single degree of freedom in vertical motion is considered here. Gust design by the discrete gust approach and also by a spectral approach are considered. Then by comparison of results, spectral design values are deduced from the discrete gust design values that have been used in the past.

The incremental acceleration in g units of the rigid body due to discrete gust encounter is given by

$$\Delta n = \frac{a\rho_0 SV_e}{2W} U_{de} K_g \tag{4}$$

where K_g is the gust alleviation factor which depends on $\mu_g = 2W/a\rho cgS$, the aeroplane mass parameter (*see* ref. 5).

From ref. 6, it may be shown that the transfer function $|H(\omega)|^2$ for vertical acceleration is given by

$$|H_{\Delta n}|^2 = \left(\frac{4V}{c_0 g \mu_0}\right)^2 \frac{k^2}{(2F/\mu_0)^2 + [k + (2G/\mu_0)]^2} \cdot \frac{1}{1 + 2\pi k}$$

where $\mu_0 = 4\mu_g$, and $k = \omega c_0/2V$. For use here, the spectral eqn. (8) given in the Appendix may be put in the form

$$\phi(k) = \frac{2L}{c}\phi(L\Omega) = \frac{\sigma^2}{\pi(2L/c)^{2/3}} \frac{(2L/c)^{5/3}\{1 + \frac{8}{3}[1{\cdot}339(2L/c)k]^2\}}{\{1 + [1{\cdot}339(2L/c)k]^2\}^{11/6}}$$

Note that care has been exercised here to put H and ϕ in forms so as to make subsequent results condense as much as possible into single non-dimensional type curves, rather than into a family of curves. The spectral equation for Δn is then

$$\phi_{\Delta n}(k) = |H_{\Delta n}(k)|^2 \phi(k)$$

Values of A and N_0 as found from $\phi_{\Delta n}$ are found to be

$$A = \frac{a\rho SV}{2W}\left(\frac{c}{2L}\right)^{1/3} B \tag{5}$$

$$N_0 = \frac{2V}{c} N_{0_1} \tag{6}$$

where B and N_{0_1} are shown in Fig. 3. The near invariance of B and N_{0_1} to L/c is to be noted.

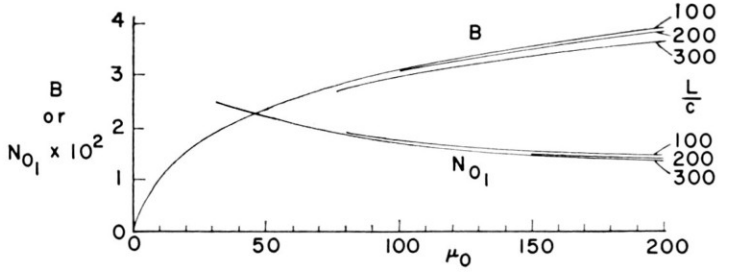

FIG. 3 — B and N_{0_1} curves

With the parameter $\Delta x/\Delta\sigma_c$ as shown in Fig. 1 in mind, let Δx be Δn; then eqn. (4) divided by $\sigma_{\Delta n} = A\sigma_c$ gives

$$\frac{\Delta n}{A\sigma_c} = \frac{\rho_0 V_e U_{de}}{\rho V \sigma_c}\left(\frac{2L}{c}\right)^{1/3}\frac{K_g}{B} \tag{7}$$

From Fig. 3 and the K_g curve of ref. 5, the curve shown in Fig. 4 follows. The close similarity of this curve with Fig. 2 is noted. Thus, the results shown in Fig. 4, based solely on rigid body response considerations, but which

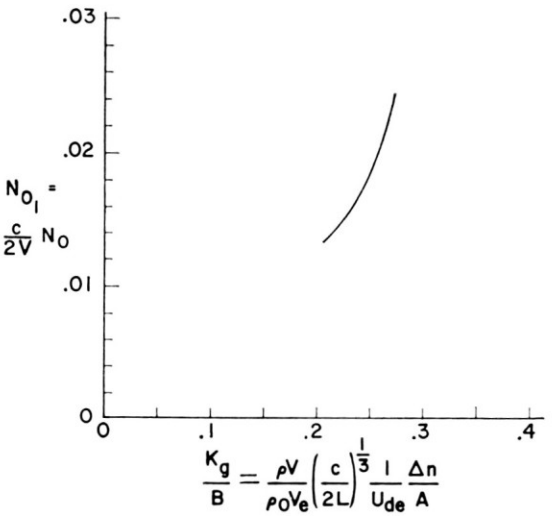

FIG. 4 — N_{0_1} versus $\Delta n/A$ as based on combined discrete-gust and spectral analysis

considerations have formed the basis for gust design for many years, may prove quite helpful in establishing the design boundary curve of Fig. 2. As an illustrative indication of possible limits on $\Delta x/A$ and N_0, consider eqns. (6) and (7). Suppose $\rho = \rho_0$, $V = V_e$, take $U_{de} = 50$, and choose $K_g/B = 0{\cdot}26$ and $N_{0_1} = 0{\cdot}021$ as representative values; eqn. (7) indicates the following

$\frac{2L}{c}$	$\frac{\Delta n}{A}$	$\frac{\Delta n}{A\sigma_c}$ (for $\sigma_c = 3$)
100	60·2	20·1
200	76·1	25·4
300	87·2	29·1
400	95·7	31·9

while eqn. (6) yields

$\frac{2V}{c}$	N_0
20	0·42
30	0·63
40	0·84
50	1·05

The values of $\Delta n/A$ and N_0 are noted to confirm the significant design range shown in Fig. 2, and the $\Delta n/A\sigma_c$ values are seen to fall in the upper or design range of Fig. 1.

These example numbers bring out the importance of knowing realistic values of L and σ_c. A means for obviating the necessity to specify L appears possible, however, and the essential idea for this possibility is given in the discussion at the end of the Appendix.

Another observation of interest can be derived from the spectral results of this section. Representative plots of $k\phi_{\Delta n}(k)$ are shown in Fig. 5; the

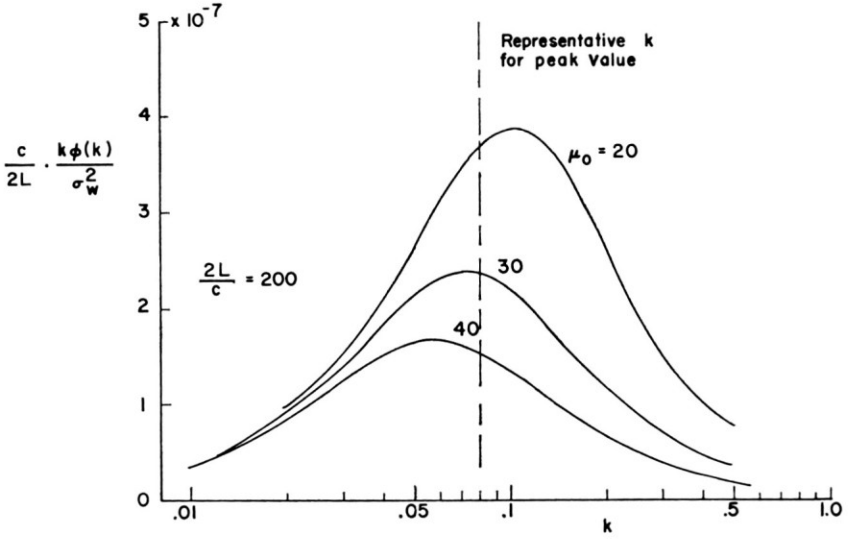

FIG. 5 — Distribution of $\sigma^2_{\Delta n}$ with frequency

curves have the significance that they show the distribution of $\sigma_{\Delta n}$ with frequency (*see* discussion associated with Fig. 7 in the Appendix). It is noticed that the curves all tend to peak in the vicinity of $k=\omega c/2V=0{\cdot}08$, thus indicating that frequency components in this neighbourhood contribute chiefly to the value of $\sigma_{\Delta n}$. The value of $k=0{\cdot}08$ is associated with a gust

wavelength of

$$\lambda = \frac{2\pi}{\Omega} = \frac{2\pi V}{\omega} = \frac{\pi c}{k}$$

$$\cong 40c$$

One quarter of this wavelength indicates a 'gust gradient' distance of

$$H = 10c$$

From this consideration it might be expected that acceleration records obtained in flight would show a predominant frequency component. Indeed this has been the case, because for years in the deduction of U_{de} there has been a preponderance of information appearing at wavelengths which appeared to be connected with the aeroplane size; specifically it became quite common to show that most of the gusts encountered tended to have gust gradient distances in the neighbourhood of 10 chords. Thus the spectral consideration made here appears to give a remarkable corroborative explanation of why these gradient distances have appeared to be favoured in flight data results which are analysed on a U_{de} basis.

5. Concluding Remarks and the Need for Consistency

As was mentioned in the body of the paper the design technique advanced here is analogous in certain respects to the discrete-gust design approach. In the discrete-gust case the gust intensity U_{de} and the gust gradient distance H are specified. In this spectral approach σ_c and L are tacitly fixed; further, all aeroplanes are treated alike just as in the discrete-gust case. Many improvements are found, however, chief among these being the fact that the spectral approach allows the various degrees of freedom of the aircraft to be taken into account in a rational way, and explicit consideration is given to the frequency of gust encounter as reflected through N_0.

Other comments not directly connected to the developments given herein, but which are related to spectral studies in general, are mentioned for consideration. There is a lack of consistency in the way flight data are gathered and presented by various countries and even by different investigators in any one country. A comparison or integration of data is hence very difficult or impossible to make. The plea is made, therefore, that we all ought to get together and agree on procedures which allow for the gathering, processing and presenting of data in a consistent, more meaningful fashion. Even the numerical spectral analysis procedures differ widely, and many of these procedures distort the data in a way that is not fully appreciated. Misleading or erroneous interpretation of the data may result. Along with the develop-

ment of spectral design procedures a promising improved way has been developed for deducing spectra which appears to be free of many of the shortcomings found in commonly used methods. This procedure should be available soon.

The question of how to resolve the scale L still remains; we really do not know at the moment whether it tends to be a constant value and if so what this value is, or whether it varies in differing turbulence conditions. The difficulty in measuring long wavelength components is the chief stumbling block in the establishment of L. We repeat here a point made in ref. 1. More attention should be paid to the instrumentation used in flight tests and what can be expected of it. A simple evaluation procedure that should be used, but which does not seem to have been followed, is the following. Flight tests of the instrumented aeroplane should be made in still air, both for the conditions of level flight and with deliberate pull-up and push-down manoeuvres; these flights should be of at least 4 minutes duration. The records should then be evaluated in the same manner as if turbulence has been encountered, to see if the vertical velocity time history evaluates to zero, as it should. Any residual trace that appears serves to indicate instrumentation limitations, and possibly what low frequency contaminations are likely to be found in the gust records. A guide would then be available to select appropriate low frequency filtering devices in the record evaluation procedures.

Appendix

Gust spectra and L values

The spectrum advocated here is that associated with isotropic turbulence and due to von Kármán, specifically

$$\phi(L\Omega) = \frac{\sigma_w^2}{\pi} \frac{1+\frac{8}{3}(1{\cdot}339L\Omega)^2}{[1+(1{\cdot}339L\Omega)^2]^{11/6}} \tag{8}$$

where σ_w is the r.m.s. value of gust velocity, and L is the turbulence scale. A plot of the equation is given in Fig. 6, and an associated plot of $L\Omega\phi$ is given in Fig. 7. This latter figure is significant in that it shows the contribution of the various frequency components to the mean square value σ^2; to see this, write

$$\sigma^2 = \int_0^\infty \phi(L\Omega)\,\mathrm{d}(L\Omega)$$

$$= \int_0^\infty L\Omega\phi(L\Omega)\,\mathrm{d}z$$

where $\mathrm{d}z = \mathrm{d}(L\Omega)/L\Omega$, or $z = \log L\Omega$. Thus with a semi-log plot with $L\Omega$ the

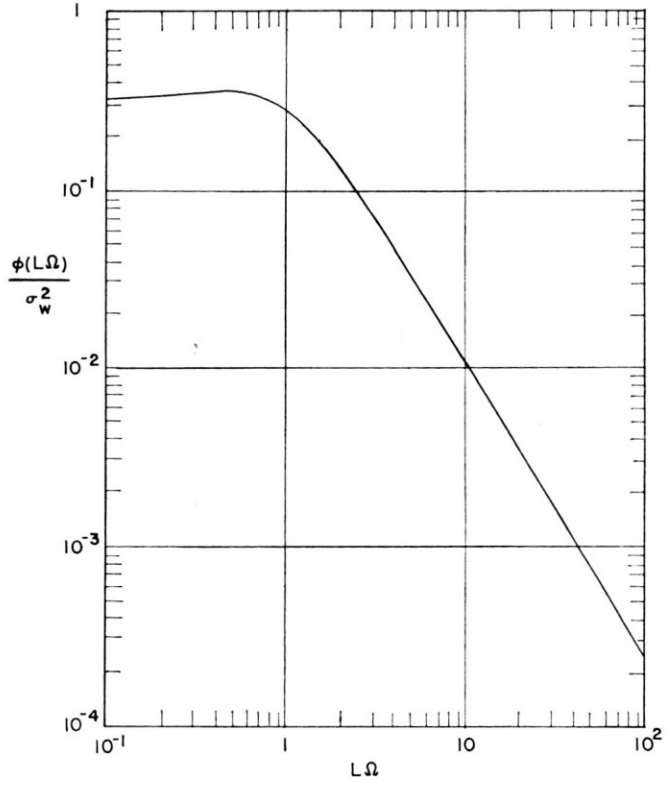

FIG. 6 — Spectral function due to von Kármán

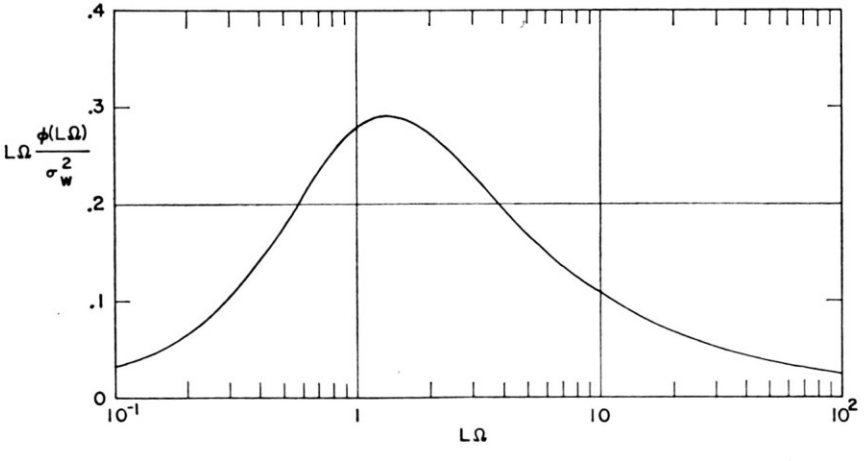

FIG. 7 — Distribution of σ^2 with frequency

log scale, the product $L\Omega\phi$ becomes a distribution curve indicating the distribution of σ^2 to the various frequency components.

The value of L to be used in design is at present uncertain, with estimates ranging from 500 to 5000 feet. A quantity that has much significance in establishing L is the truncated value of r.m.s. gust velocity defined by

$$\sigma_1^2 = \int_{(L\Omega)_1}^{\infty} \phi(L\Omega)\,\mathrm{d}(L\Omega) \tag{9}$$

The insertion of eqn. (8) into this integral leads to the results shown in Fig. 8. In application to flight data, values of σ_1, σ_w, and L must be such as to satisfy the curve of this figure. In general, σ_1 is established with good accuracy but

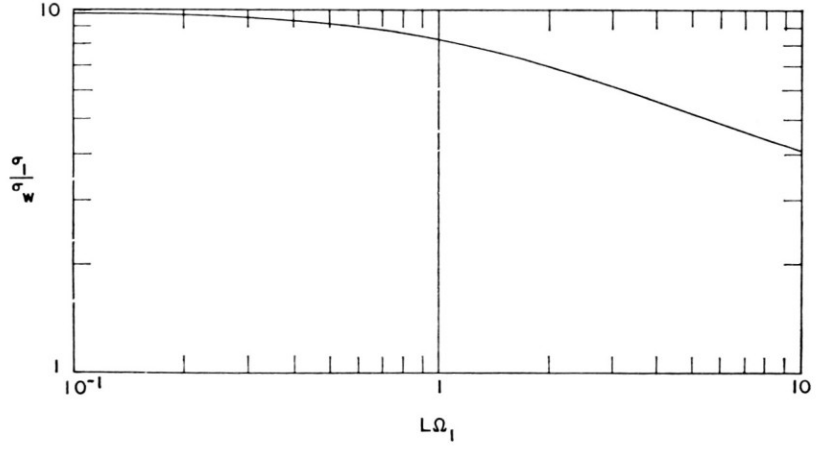

FIG. 8 — Truncated r.m.s. value σ_1

σ_w is questionable because of the presence of uncertain long wavelength components in the gust velocity records. Thus since σ_1/σ_w is uncertain, the deduced L is also. Stated in other terms, for a given σ_1, there can be many combinations of σ_w and L which when substituted in eqn. (8) give ϕ curves which fit the flight data equally well. This fact can be demonstrated in specific terms as follows. For eqn. (8), the result obtained from eqn. (9) for $(L\Omega)_1 > 3$ is

$$\sigma_1^2 = \frac{0{\cdot}782\sigma_w^2}{(L\Omega)_1^{2/3}} \tag{10}$$

With this equation and the fact that $\phi(\Omega) = L\phi(L\Omega)$, eqn. (8) may be rewritten

$$\phi(\Omega) = \frac{\sigma_1^2(\Omega_1)^{2/3}}{0{\cdot}782\pi} \frac{L^{5/3}\left[1+\frac{8}{3}(1{\cdot}339L\Omega)^2\right]}{\left[1+(1{\cdot}339L\Omega)^2\right]^{11/6}} \tag{11}$$

With Ω_1 arbitrarily chosen as 0·003, this equation yields the results shown in Fig. 9. All curves have unit area beyond $\Omega = 0{\cdot}003$ regardless of L; or, if ϕ, not $\phi(\Omega)/\sigma_1^2$, is plotted against Ω, all curves would yield the same truncated

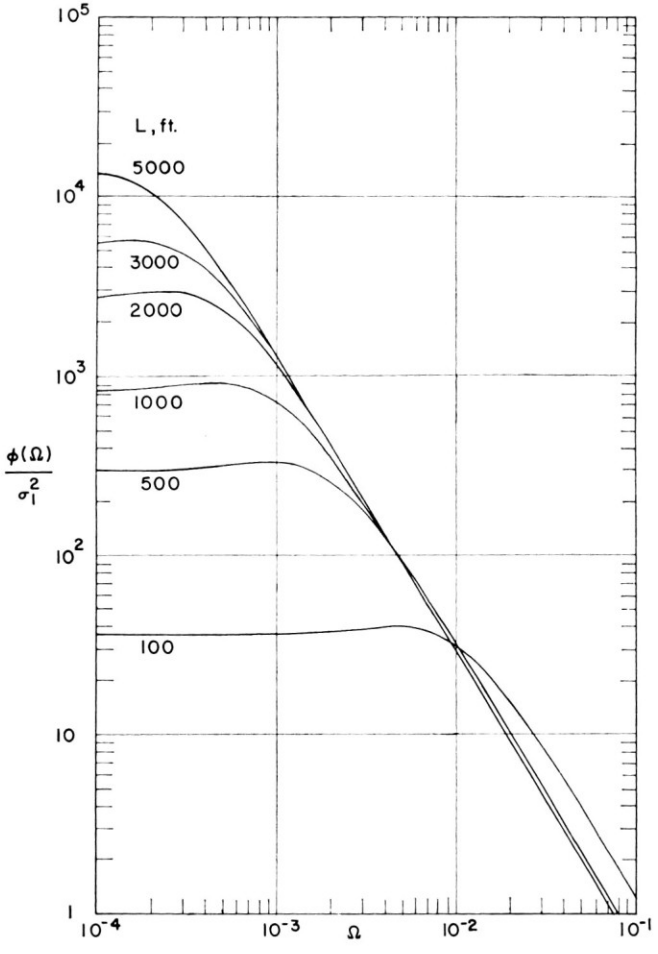

FIG. 9 — Spectral plots equal truncated values σ_1 beyond $\Omega = 0{\cdot}003$

value σ_1^2. For low Ω, however, appreciable difference is noted in the level of the curves for different L. This lower range is the range where evaluation of flight test data is difficult or impossible at present.

The use of ϕ curves in the form shown by Fig. 9 may become useful and appropriate. In general, the value of A is found to depend on the value of L used. However, if eqn. (11) or the ϕ curves of Fig. 9 are used, then the sen-

sitivity to L can be virtually eliminated. Specifically, suppose eqn. (10) is combined with eqn. (2) by eliminating σ_w. The result can be written

$$\sigma_x = A\sigma_w = A\frac{(L\Omega_1)^{1/3}}{0{\cdot}885}\sigma_1$$

$$= A_1\sigma_1$$

This newly defined structural parameter A_1, involving the truncated value σ_1, is found to be practically insensitive to L; that is, actual calculations indicate that the product $AL^{1/3}$ is nearly constant. Thus, the use of a spectral curve with a specified truncated value may prove to be a worthwhile direction to go, since it minimises the need for establishing and designating a design value of L. Possible methods of improving the ability to deduce L are being developed, however, in the continuing research study.

References

(1) Houbolt, J. C., 'Interpretation and Design Application of Power Spectral Gust Response Analysis Results.' AIAA/ASME Seventh Structures and Materials Conference, Cocoa Beach, Florida, April 18–20, 1966.

(2) Houbolt, J. C., 'Preliminary Development of Gust Design Procedures Based on Power Spectral Techniques', Volume I and II. Technical Report AFFDL–TR–66–58, May 1966.

(3) Houbolt, J. C., 'Low Altitude High Speed Flight — Impact on Aircraft Structures', NAECON, Dayton, Ohio, May 1966.

(4) Houbolt, J. C., Steiner, R., Pratt, K. G., 'Dynamic Response of Airplanes to Atmospheric Turbulence Including Flight Data on Input and Response.' NASA Tech. Rept. TR R–199, June 1964.

(5) Pratt, K. G., Walker, W. G., 'A Revised Gust-Load Formula and a Re-Evaluation of V–G Data Taken on Civil Transport Airplanes from 1933 to 1950', NACA Rept. 1206, 1954.

(6) Houbolt, J. C., Kordes, E. E., 'Structural Response to Discrete and Continuous Gusts of an Airplane Having Wing-Bending Flexibility and a Correlation of Calculated and Flight Results', NACA Rept. 1181, 1954.